Optical configuration of fundus camera based on inner focusing manner

Haishui Ye (叶海水)*, Zhishan Gao (高志山), Ting Luo (罗 婷), and Yang Huang (黄 阳)

School of Electronic Engineering and Optoelectronic Techniques,
Nanjing University of Science and Technology, Nanjing 210094, China
**E-mail: yhs.1986@163.com*

Received December 28, 2009

The fundus camera used in imaging retina includes two parts: fundus imaging path with a positive focusing lens and annular Kohler illuminating path. We present a pupil joint equation and a focus equation based on the internal focusing manner to analyze its configuration. Using these equations, the configuration of the camera is given in detail. The design result of the fundus imaging path shows compact initial configuration at a total length of about 123 mm. The focusing range is –10−10 diopter, and the movement of the focusing lens is nearly linear at displacement of more than a sub-millimeter per diopter.

OCIS codes: 170.0110, 170.4460, 170.1610, 120.4570.
doi: 10.3788/COL20100807.0689.

The fundus camera is an optical system that can be used in imaging fundus tissues. It plays an important role in contemporary ophthalmic diagnosis, such as macular degeneration. Considering the complexity and speciality of the structure of the human eye, the fundus camera consists of both imaging and illuminating paths. The former receives ray scattered by fundus tissues and with a special path to realize fundus imaging; the latter provides enough illumination to the imaging path to offset low luminance resulting from the low scattering[1] of fundus tissues.

The cornea located at the outer part of the human eye has a high reflectance. It greatly affects fundus tissue imaging. Therefore, controlling its reflectance is important in fundus camera design. According to Ref. [2], a special annular Kohler illumination manner has been applied in the fundus camera. The irradiance into fundus tissue should be controlled below the maximum permissible safety exposure (MPE) during fundus imaging. Uniform illumination[3] is required in the illumination path design to ensure comfort when illuminated by light at near-infrared wavelength.

Two requirements should be considered during the process of imaging path design: it should be pupil-jointed (i.e., the position of the pupil entrance of the camera is located at the eye's pupil), and it should allow either near-sight or far-sight focus. Traditional designs consisted of moving the eyepiece, objective lens or charge-coupled device (CCD)[4], and the entire imaging group[5]. The moving eyepiece brings various positions onto the conjugate image, thus limiting Kohler illumination. Additional adjustment systems should be introduced into the illumination path because of the moving black dot[2,3], which could then remove the ghost image in the eyepiece. The manner of moving the objective lens or CCD could avoid the disadvantages mentioned earlier, but it also results in shifting conjugated positions and swayed images. Moving the entire lens group shares the speciality of the simple structure, but it also fails to acquire a stationary image.

A fundus camera using the inner focus method is proposed in this letter, which could guarantee stationary images during focusing. We will discuss how the illumination and imaging path should be chosen for the fundus camera design. The corresponding configuration is also calculated.

The imaging path consists of eyepiece L_2, focusing lens L_3, and objective lens L_4, as shown in Fig. 1. The eyepiece connects the human eye with the imaging system. The focusing lens is located between the eyepiece and the imaging lens. Its movement allows the fundus to be refocused when illuminated by the beam of near-infrared wavelength, and reduces the incident height of objective lenses, such as field lenses. The objective lens located at the end part of the fundus camera connects with the CCD and is composed of the image receiver of the whole fundus camera.

The illuminating path consists of a collecting lens L_6, condenser lens L_5, and eyepiece L_2. It shares the eyepiece with the imaging path, as shown in Fig. 2. The annular Kohler illumination method could effectively avoid stray light from the reflectance of the cornea and improve signal-to-noise ratio (SNR) due to its higher reflectance at the center as opposed to the edge of the cornea.

The central part of the mirror with a central hole permits the imaging light to pass through the camera. The edge of the reflecting mirror allows the illuminating light to pass through and enter the pupil from the edge of the cornea, thus successfully realizing the separation of the illuminating and imaging paths.

Fundus tissues and CCD form a conjugate imaging pair in the fundus camera, as shown in Fig. 1. The imaging system, consisting of intraocular optical system, eyepiece L_2, focusing lens L_3, and objective lens L_4, satisfies

$$\frac{1}{(d_{34}-c_4)}-\frac{1}{(f_2'-d_{23})}=\frac{1}{f_3'}, \tag{1}$$

$$c_4=(1-\beta_4)f_4', \tag{2}$$

where d_{34} denotes the distance between the objective lens

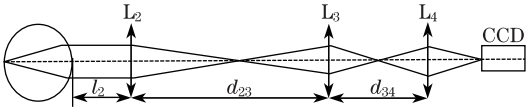

Fig. 1. Fundus imaging path.

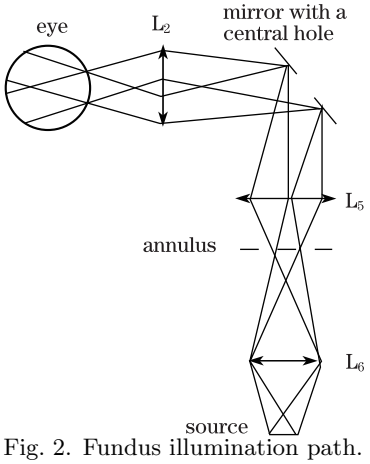

Fig. 2. Fundus illumination path.

and the focusing lens, d_{23} denotes the distance between the focusing lens and the eyepiece, f_2', f_3', and f_4' denote the focal lengths of the lenses L_2, L_3, and L_4, respectively, and β_4 denotes the lateral magnification of the Lens L_4.

According to the principle of reversibility, we assume that the entrance pupil of the imaging path is located at the objective lens. The position of the corresponding exit pupil should be the same as in the pupil of the human eye; otherwise, it will lead to vignetting due to limited aperture, and subsequently, direct reduction of the luminous flux received by the CCD. Therefore, according to design requirements, the conjugate image of the human eye pupil formed by the eyepiece was placed as an image at the surface of objective lens, which could be written as

$$\frac{1}{d_{34}} - \frac{1}{c_2 - d_{23}} = \frac{1}{f_3'}, \tag{3}$$

with

$$c_2 = \frac{f_2' l_2}{l_2 + f_2'}, \tag{4}$$

$$c_2' = \frac{f_2' l_2}{l_2 + f_2'} - f_2' = \frac{-f_2'^2}{l_2 + f_2'}, \tag{5}$$

where l_2 denotes the distance between eyepiece and cornea, as shown in Fig. 1. Equations (3)−(5) consist of pupil joint equations, and d_{34} could be determined by combining Eqs. (1) and (3):

$$d_{34} = \frac{2f_3' + c_4 \pm \sqrt{c_4^2 + \frac{4c_4}{c_2'} f_3'^2}}{2}. \tag{6}$$

In the study, d_{34} is an important parameter relative to the configurations of focusing lens L_3, objective lens L_4, and eyepiece L_2. According to Eq. (6), the distance d_{34} relates to f_3', f_2', the exit pupil distance l_2, and parameter c_4. Thus, after analyzing their impact on d_{34}, the choices for the lens group structure in the imaging path could be determined.

The eyepiece has a short focal length, small relative aperture, and a large field of view (FOV). The exit pupil distance varies with the change in the eyepiece structure. Therefore, depending on focal length, the eyepiece is larger or smaller than the exit pupil distance.

When the focal length of the eyepiece is larger than the exit pupil distance (i.e., $f_2' > -l_2$ and parameter $c_2 < 0$), only the positive lens could be used as the focusing lens. In such condition, according to Eq. (3), the positive d_{34} and negative f_3' can lead distance d_{23} to a negative value.

The other condition is when the focal length of the eyepiece is smaller than the exit pupil distance (i.e., $f_2' < -l_2$). If $c_4 > 0$, $c_2' > 0$, the square root result for Eq. (6) is larger than c_4, then we have

$$d_{34\_1} > f_3' + c_4, \tag{7}$$

$$d_{34\_2} < f_3', \tag{8}$$

where d_{34_1} and d_{34_2} are two solution of d_{34}. If the negative lens is chosen as the focusing lens, only one of the solutions for d_{34} is practical; usually, its value is small. The entrance pupil of the entire imaging path is located at the surface of the objective lens, and the position of the corresponding exit pupil is the same as that of the location of the human eye pupil. Therefore, the lateral magnification between the human eye pupil and the objective lens surface is described as

$$\beta_{32} = \frac{d_{34} - f_3'}{f_3'} \frac{f_2'}{l_2 - f_2'} > \frac{c_4}{f_3'} \frac{f_2'}{l_2 - f_2'}. \tag{9}$$

Usually, in the imaging path, the value of c_4 is far larger than f_3', and the value of the lateral magnification β_{32} is large. Considering that the diameter of the exit pupil is constrained by less than 4 mm, the imaging objective is certain to have a large relative aperture, which increases the complexity of the objective lens structure.

Two practical solutions of d_{34} exist if the positive lens is used as the focusing lens. However, one is larger than the other, yet both have their own limitations. The former leads to a large relative aperture of the objective lens, while the latter easily makes different parts of the lens groups to be in contact with each other during focusing.

In summary, the design of the eyepiece is applied to the structure of general eyepiece. It has short focal length, small relative aperture, and large FOV. The negative lens cannot be used as the focusing lens once the focal length of the eyepiece is larger than the exit pupil distance. However, the positive focusing lens leaves an appropriate space for the different parts of lens groups and can increase movement during focusing adjustment, making the process easy to realize. When the focal length of the eyepiece is less than the exit pupil distance, either a positive or a negative focusing lens could limit the design, or result in failures in focusing adjustments due to the minimum space among different parts of lens groups.

Focusing is required in the imaging path design to realize fine-focusing for different types of eyesight.The inner

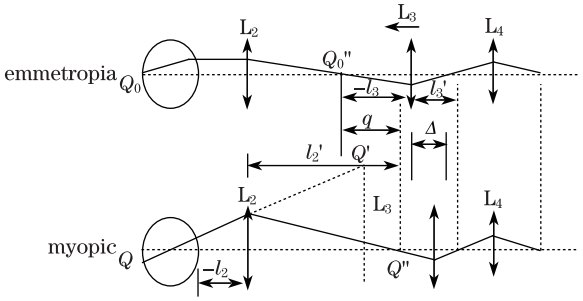

Fig. 3. Focusing of fundus camera.

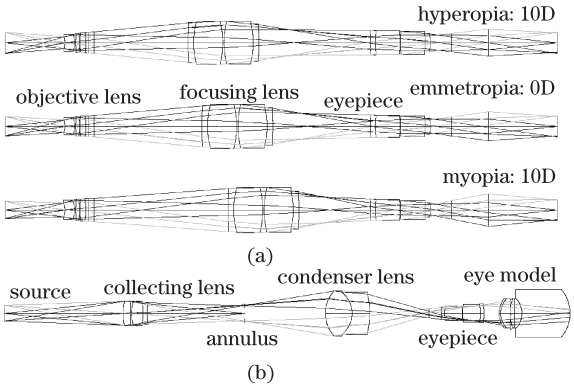

Fig. 4. (a) Imaging path corresponding to myopia (–10D), emmetropia (0D), and hyperopia (10D); (b) illumination path of fundus camera.

focus manner is proposed in this letter. A positive focusing lens is inserted between the eyepiece and the objective lens. Fine-focusing is carried out by moving the focusing lens, as shown in Fig. 3.

In such a focusing manner, the movement of the focusing lens compensates for the shift of retinal conjugate image of different eyesight after the eyepiece. This allows the fixed CCD to gain clear conjugate images. Only a small change in magnification is presented during the focusing process.

A value of diopter D is usually used to show the eyesight of patients in clinical ophthalmology. The positive and negative values of D denote hyperopia and myopia, respectively. If the conjugate image of some points at the fundus is $1000/D$ away from cornea, we have the image distance l_2' next to the eyepiece described as

$$\frac{1}{l_2'} - \frac{1}{\frac{1000}{D} + l_2} = \frac{1}{f_2'}. \tag{10}$$

The symbol q is defined as

$$q = l_2' - f_2'. \tag{11}$$

We introduce the Gauss formula to obtain

$$\frac{1}{l_3'} - \frac{1}{l_3} = \frac{1}{f_3'}, \tag{12}$$

$$\frac{1}{l_3' + \Delta} - \frac{1}{l_3 - q + \Delta} = \frac{1}{f_3'}, \tag{13}$$

as shown in Fig. 3, where Δ denotes the movement of the focusing lens L_3, l_3 denotes the distance beetween the point Q_o'' and lens L_3, and l_3' denotes the distance between the corresponding imagine point and lens L_3.When the focusing lens L_3 moves to the left, Δ gains a positive value. Point Q in the fundus gains its own image at point Q'' after passing through eyepiece L_2. If the image point

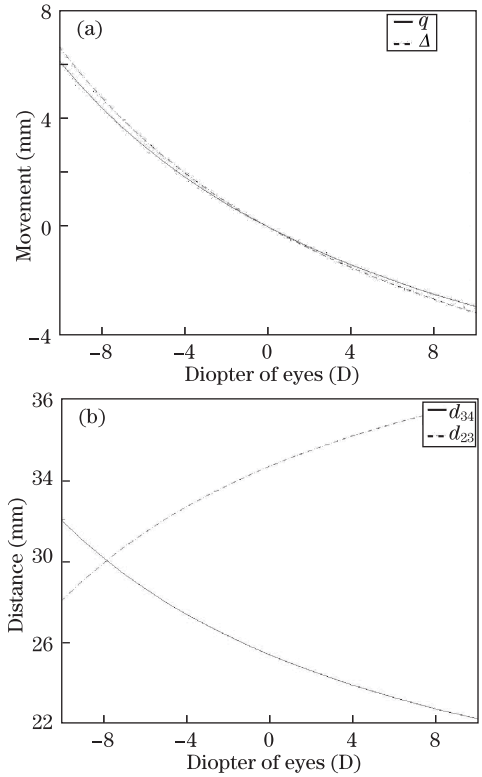

Fig. 5. (a) q and Δ versus D of eyes, (b) d_{23} and d_{34} versus D of eyes.

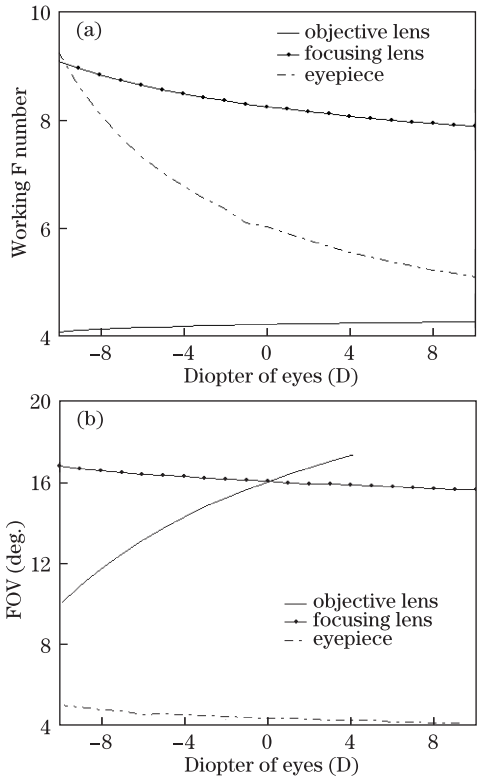

Fig. 6. (a) $F/\#$ and (b) FOV of lens groups.

Q'' is located at the right of the normal fundus image Q''_o, q achieves a positive value; otherwise, it is negative. By simplifying Eqs. (12) and (13), we obtain the corresponding focusing equations:

$$\frac{\Delta}{l'_3+\Delta}=\beta_3\frac{-q+\Delta}{l_3-q+\Delta}, \tag{14}$$

$$\beta_3=l'_3/l_3, \tag{15}$$

where β_3 denotes the lateral magnification of the lens L_4. Solving Eq. (14), we have movement Δ of focusing lens as

$$\Delta=\frac{q-\frac{f'_3}{\beta_3}+\beta_3 f'_3\pm\sqrt{(q-\frac{f'_3}{\beta_3}+\beta_3 f'_3)^2-4\beta_3 q f'_3}}{2}. \tag{16}$$

According to Eq. (16), it is easy to know if Δ is determined by f'_3, β_3, and q. Two movement curves are presented by the focusing lens. However, neither could satisfy the requirements of focusing. Mainly, judging the practical curve is guided by the movement of the focusing lens, which should be less than its distance with either the objective lens or eyepiece. Equation (16) can also obtain the focusing range of the entire imaging path:

$$\left(q-\frac{f'_3}{\beta_3}+\beta_3 f'_3\right)^2\geq 4\beta_3 q f'_3. \tag{17}$$

It is possible to gain the focusing range of the imaging path once Eqs. (10), (11), and (17) are combined. Our design of the fundus camera gives a focusing range of –10−10 diopterv, which is suitable for people with medium myopia or hypermetropia.

Figure 4(a) describes the initial structure of the imaging path, while Fig. 4(b) describes the initial structure of the illumination path. The focal length of the focusing lens and eyepiece was 20 mm, and the lateral magnification of the focusing lens was 3.7321 for emmetropia. The distance between the eyepiece and the cornea was 10.15 mm, while the total length of the fundus camera was 123.4 mm, at which its conformation is highly compact.

No strict restrictions were presented for the aberration in the illumination path[6], and therefore the design of the collecting lens and condenser lens adopted a three-piece lens and cemented doublet lens, respectively. The inner diameter of the annular stop was 4.4 mm while the external diameter was 10 mm. The illumination path and imaging path was separated, and the illumination efficiency were 31.6%.

Figure 5(a) describes the movement of the focusing lens while Fig. 5(b) shows the distances between lens groups. From myopia to hyperopia, the focusing lens moved towards the objective lens, and the corresponding movement of the focusing lens at 1 D was about 0.7 mm.

Figures 6(a) and (b) describe the working F number ($F/\#$) and FOV of lens groups of the imaging path during focusing. From myopia to hyperopia, the $F/\#$ and FOV of objective lens[7] increased continuously, obtaining medium relative aperture and large FOV. The $F/\#$ and FOV of the focusing lens decreased as diopter increased, with the latter decreasing slowly. The focusing lens has a simpler structure compared with the objective lens due to smaller relative aperture. The $F/\#$ and FOV of eyepiece also decreased continuously as the diopter increased. Overall, due to small FOV and relative aperture, the method was easily designed.

The imaging and illumination paths were connected by a mirror with a central hole, which allows the outer part of pupil to be illuminated. Hence, by using such method, the fundus tissue could be illuminated as well, leaving the center of pupil not illuminated, and subsequently, allowing the imaging path to pass through the design. The primary reflectance at the eyepiece was greater than the quantity of the scattered fundus tissue, and thus the generated ghost image affected the quality of the fundus imaging. The black dot was applied to remove the ghost image, thus improving the SNR of the system.

In conclusion, we discuss how illumination and imaging path should be chosen in the design of a fundus camera. We propose the corresponding pupil joint and focus equations based on the inner focus method. Then, the initial structure is calculated. Such approach is not only practical in the identification of myopia and hyperopia with medium diopters, it also offers compact configuration beneficial to miniaturizing the entire fundus camera. The system based on the inner focus method ensures stationary images, and the corresponding movement of the focusing lens at 1 D is about 0.7 mm. Therefore, its mechanical structure is easy to realize.

This work was supported by the National Natural Science Foundation of China (Nos. 60977008 and 60678048), the Natural Science Foundation of Jiangsu Province (Nos. BK2007207 and BS2007061), and the "Six Elites Peak" of Jiangsu Province.

References

1. F. C. Delori and K. P. Pflibsen, Appl. Opt. **28,** 1061 (1989).
2. E. DeHoog and J. Schwiegerling, Appl. Opt. **48,** 221 (2009).
3. E. DeHoog and J. Schwiegerling, Appl. Opt. **47,** 6769 (2008).
4. Z. Wang and Y. Xu, Optics and Precision Engineering (in Chinese) **16,** 1567 (2008).
5. C. Zhang, "Research of photoelectric fundus camera" Master Thesis (Shandong University, Ji'nan, 2004).
6. C. Li, B. Jiang, M. Xia, S. Cheng, and L. Xuan, Acta Opt. Sin. (in Chinese) **28,** 2245 (2008)
7. L. Ai, F. Yuan, and Z. Ding, Acta Opt. Sin. (in Chinese) **28,** 1930 (2008)